University of Wah Journal of Science and Technology Vol. 8 (2024),PP 34-51.
ISSN: 2523-0123 (Print) 2616-4396 (Online)

University of Wah
Journal of Science and Technology

www.uow.edu.pk

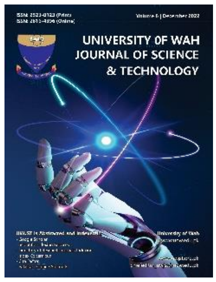

Track Mechanism Design for a Differential Drive Fire Fighting Robot

Syed Haris Shah[1] , Nasir Rahman[2] , Rizwan Alim Mufti[1] , and Muhammad Ali*[3]

[1]Department of Mechanical Engineering, PIEAS, Nilor, Islamabad

[2] Department of Electrical Engineering, PIEAS, Nilor, Islamabad

[*3]Department of Physics and Applied Mathematics, PIEAS, Nilor, Islamabad

*Corresponding author email: muhammadali@pieas.edu.pk

Abstract

Rescue missions and disaster management expose human life to risk further elevating the catastrophe. Robotics and automation can play pivotal role to provide solutions through Unmanned Ground Vehicles (UGV) in normal and accidental situations without posing or minimizing risk to human life. Firefighting is one of the most needed areas of disaster management where robots can expand the capability of fire hydrant to control fire in natural or manmade uneven structures in buildings, factory areas, power, chemical plants etc. Robotics and Automation engineers are working on developing robots for reducing hazards to human fire fighters. The purpose of this study is to design and develop an efficient track mechanism for a supervised tele-operated firefighting robot. The essential requirements of the subject platform were its maneuverability and negotiation over uneven terrains especially stair-like surfaces.

Keywords

Fire Fighting, Rescue Robot, Stair Climbing, Unmanned Ground Vehicle, Supervised Tele-operation

1. Introduction

Globally every industry is automating their operations. Robots and Artificial Intelligence (AI) is used to make processes faster and productions cheaper. This project aims to introduce automation in firefighting industry with two major objectives. Firstly, such projects would improve the safety standards of the firefighting industry. In firefighting industry, human lives are vulnerable while coping with huge fires and accidental situations. Automating the process can reduce the involved risks in firefighting. Instead of exposing human lives on the front line to extinguish fires, the process can be remotely supervised and executed with enhanced safety. Secondly, the aim of the project was to enhance efficacy and efficiency of the firefighting process.

While deploying human fire fighters, there are number of factors that reduce the overall efficiency for example and the general safety concerns of the personnel like physical limitations of the fire fighter to carry a limited quantity of equipment, panic due to potentially fatal environments. All these factors jeopardize the efficacy and efficiency of firefighting process. We envisaged that automating the process and remotely controlling it would iron out these issues as robot would have the capability of carrying multiple hoses, hence improving the efficiency of firefighting. Moreover, response time would not be hindered due to safety related apprehension. Hence, the overall effectiveness and efficiency of the process would be improved.

2. Literature Review

The concept of automation in the firefighting industry is deemed relatively new, with various robotic automations designs and concepts explored in literature. Over the past decade, various studies have explored the use of robotics and automation to enhance firefighting operations, some of which are referred and discussed here. One such example is the firefighting robot developed and designed to detect and extinguish fires while following a predefined path [1]. Recently studies have been published with focus on firefighting robots [2-5]. Development of firefighting root for nuclear accidents has also been presented [6]. The concept of an indoor firefighting robot with features such as fire extinguishing, assisting the trapped people by providing them with masks and other safety gadgets and surveillance of the disaster site was presented [7]. presented concept of an autonomous robot to detect the fire's location [8]. Three year ago, Sathiabalan et al. published a study of autonomous robotic fire detection and extinguishing system [9]. The design and analysis of a tracked robot driven by a single DC motor was presented [10]. The design of a small-scale firefighting robot to assist the firefighters by entering the areas which cannot be accessed by firefighters and hence could mitigate the effect of spreading of fire [11]. [12]Design and Implementation of a Robot Firefighter for Indoor Applications. Even mini robot for firefighting has been designed [13]. [14] also presented a concept of mobile robot platform. It constituted of four tracked leg articulation which moved independently. Having four independent tracks, a variable geometry track mechanism design was presented. In high traction requirements all the four tracks would be in contact with the ground while the variable geometry capabilities of the mechanism would be used for maneuverability against obstacles. In another study, the detailed kinematic modeling of the same robot was presented [15]. In another study, [16] also presented an optimal design of a tracked robot. [17] in 2018, studied the dynamics of steering of a tracked robot based on track slip and centrifugal force and computed pressure on each side of track and concrete steering offset. [18], presented the study of dynamics and stability of a tracked robot while climbing stairs. [19], presented simulation of tracked mechanism while climbing an obstacle using MSC.ADAMS in order to evaluate and optimize the chassis. [20] , presented a comparison of power losses in skid steered, wheeled, and tracked robots. The study incorporated the effect of deformable terrain.

Every mechanism has its own advantages and disadvantages subject to application area. The terrain decides which one is most suitable. It is a trade off between speed and capability to maneuver.

- **i.** Track mechanism has lower speed but effective and stable on uneven surfaces likes stairs or sandy surfaces as compared to wheeled mechanisms.
- **ii.** Moreover they are highly stable as compared to legged mechanism as far as their gait modelling and design is concern.
- **iii.** Track mechanism is also preferred due to simple design as it is less complicated to design and fabricate as compared to legged mechanism.

Our vision for a firefighting robot integrates all the concepts presented above into a single design. This study presents an advanced mobile platform for a firefighting robot with a differential drive system having capability of navigating a range of obstacles encountered in diverse environments..previously presented steering mechanism for a differential drive driven, IC engine powered firefighting robot [21]. This research is a extension of the said study.

3. Material and Methods for Design

A CAD (computer aided design) model of the track mechanism was designed in Autodesk Inventor. The key parameters kept in mind for the design were the requirements from the track mechanism in terms of the active load it would experience, the ground clearance of the chassis and the space requirement for the components to be placed in the chassis. The CAD model included the design of both the chassis and the track mechanism. Important components of the design are as follows:

3.1 Side Plates and Frame

The design considerations include best choices like balancing optimal weight, strength, and cost. Aluminum and mild steel hollow pipes are chosen with consideration of these three factors. A framed structure was preferred which composed of a frame made up of 1 inch x1.5 inches (25.4 x 38.1 mm^2) Mild Steel pipes and 5.5 inches (139.7 mm) Aluminum plate bolted on to the frame to house all the major components.

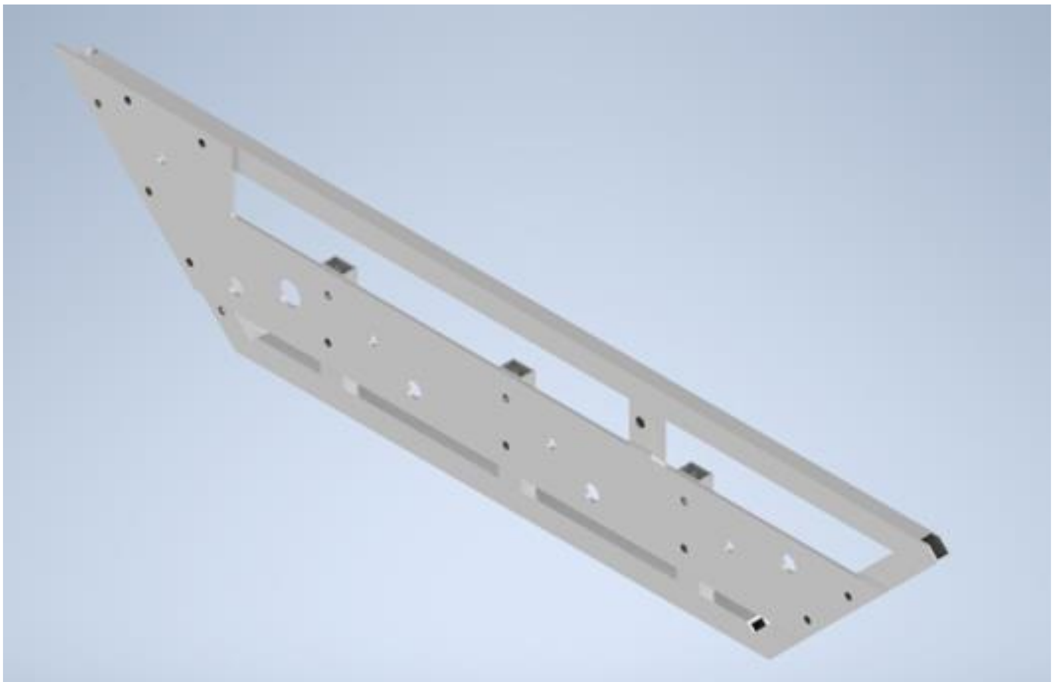

Fig. 1. *Bolted Frame and Side Plates Assembly*

M12 bolts were used to fasten the plate to the frame in shown in Figure 1. Two such assemblies formed the sides of the Chassis and were linked across using 1 inch (25.4 mm) round MS (mild steel) rods.

3.2 Idler Assembly/ Legs

The idler assembly acts as the arms of the robot. There are 6 idler assemblies in the design, 3 on either side. One end of the idler assembly is connected to the side plate via bearing so that it can rotate freely, while, the idler wheels on the other end are pressed against the belt. The labelled image of the idler assembly can be seen in Figure 2:

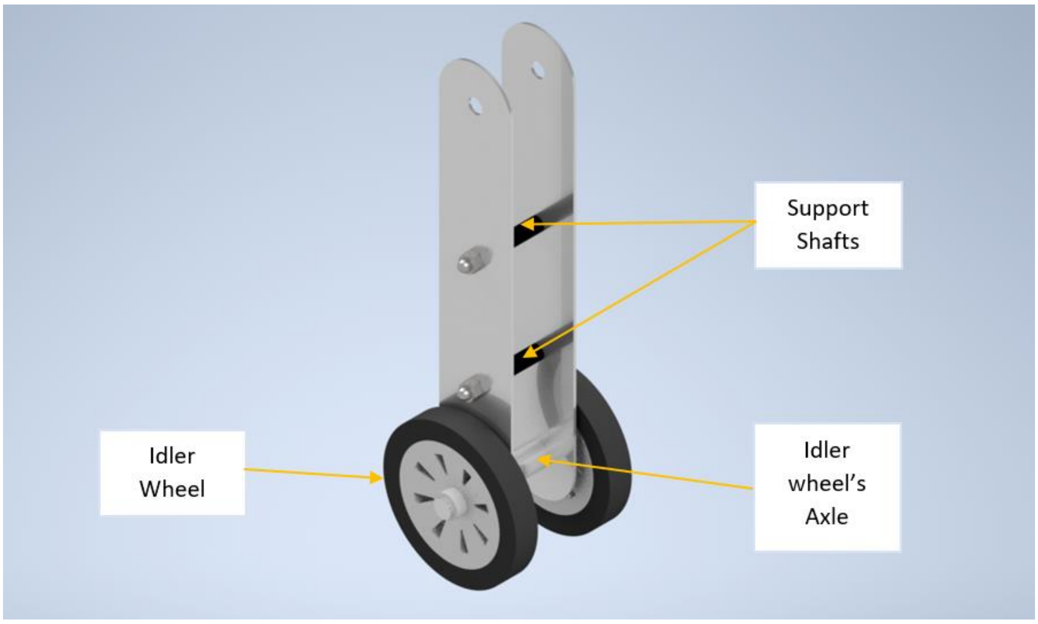

Fig. 2. *Labelled Model of Idler Assembly*

Each idler assembly consists of a pair of idler wheels. The idler wheels serve as guides for the belts and rotate as the belt moves. The space between the two wheels accommodates the protrusions from the belt so that the belt doesn't come off its intended path.

The two support shafts in the idler assembly not only serve the purpose of integrating the assembly but the lower set also acts as the shock absorber that is to be attached to the idler assembly.

3.3 Shock Absorber

Another key component in the design is the shock absorber. All the 6 legs of the robot are connected back to the main body via shock absorbers, hence, completing the suspension assembly. The labelled assembly of the shock absorber can be seen the Figure 3:

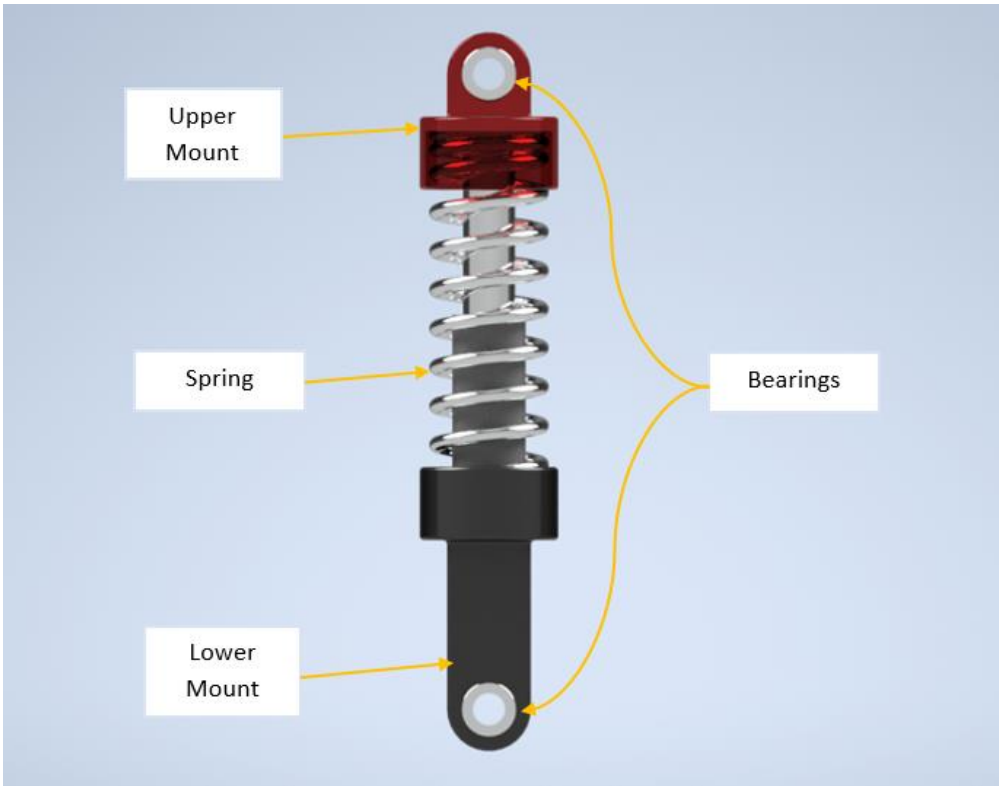

Fig. 3. *Labelled Model of Shock Assembly*

The key design component in the shock absorber is the spring. The spring here was designed in the Autodesk Inventor's Design Accelerator. The calculations for the spring were done under an active loading condition of 245.250 N, equating to an active load of 25 kg per shock. A maximum load of 400 N per spring was used, equating to 40.770 kg maximum loading condition.

4. Results and Discussion

Using a wire of 7 mm (dia) and spring of 50 mm (dia) calculations were performed in Design Accelerator. The following results were obtained from design accelerator.

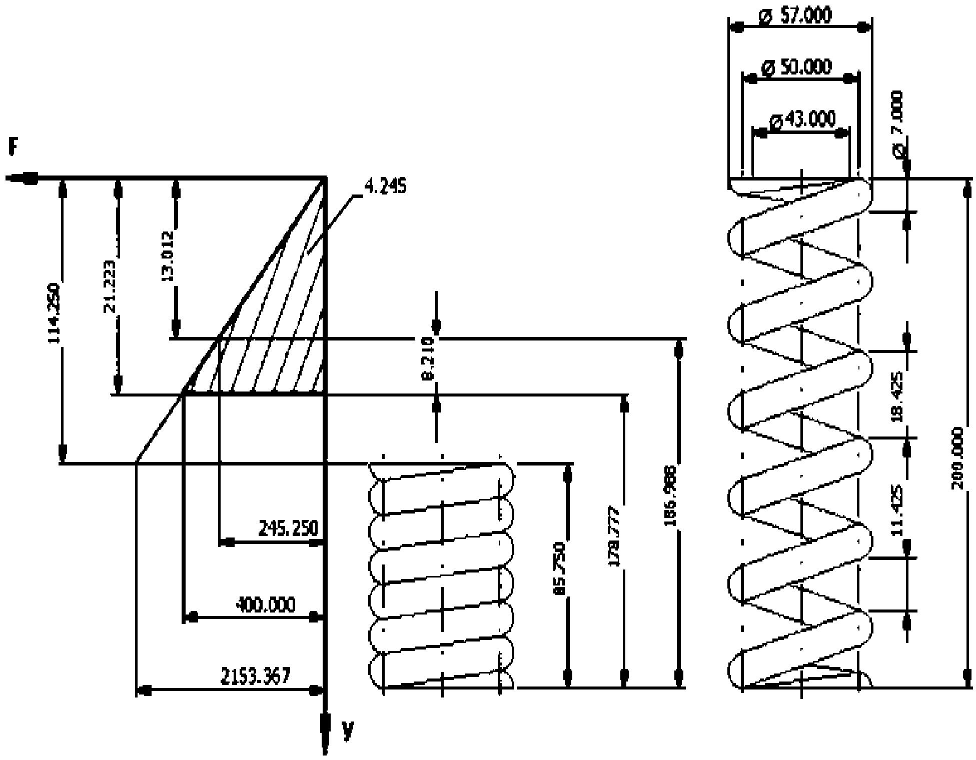

Fig. 4. *Behavior of Spring with Force Variation*

The behavior of the spring shown in Figure 4 as the force is increased from 0 N to 400 N is elaborated in the image above. Under no loading condition the spring has its free length of 200 mm. When the working load (245.250 N) is applied to the spring a compression of 13.012 mm is observed. Under the maximum loading condition of 400 N, a compression of 21.223 mm is observed. The elastic limit of the spring comes out to be 114.250 mm.

The detailed results obtained from design accelerator are tabulated below in Table 1:

Table 1: Results Obtained from Design Accelerator

Parameter	**Symbol**	**Value**
Space between Coils of Free Spring	a	11.425 mm
Pitch of Free Spring	t	18.425 mm
Stress Concentration Factor	K_w	1.000 ul
Spring Constant	k	18.848 N/mm
Min. Load Spring Deflection	s_1	13.012 mm
Total Spring Deflection	s_8	21.223 mm
Limit Spring Deflection	s_9	114.250 mm
Limit Test Length of Spring	L_{minf}	100.038 mm
Theoretic Limit Length of Spring	L_9	85.750 mm
Spring Limit Force	F_9	2153.367 N
Min. Load Stress	T_1	91.038MPa
Max. Load Stress	T_8	148.483MPa
Solid Length Stress	T_9	799.345MPa
Critical Speed of Spring	V	18.528mps
Natural Frequency of Spring Surge	f	99.583 Hz
Deformation Energy	W_8	4.245 J
Wire Length	I	2000.000 mm
Spring Mass	m	0.605 kg
Spring Check Result		Positive

4.1 Tensioner Assembly

The belt of the tracked assembly might be fitted in tensioned state under static load. However, when the robot moves, the load variation on the different wheels causes compression of the suspension assemblies. This reduces the overall loop length on which the belt was fitted initially causing the belt to loosen and come of its intended path. The tensioner assembly designed for our case is shown in the Figure 5:

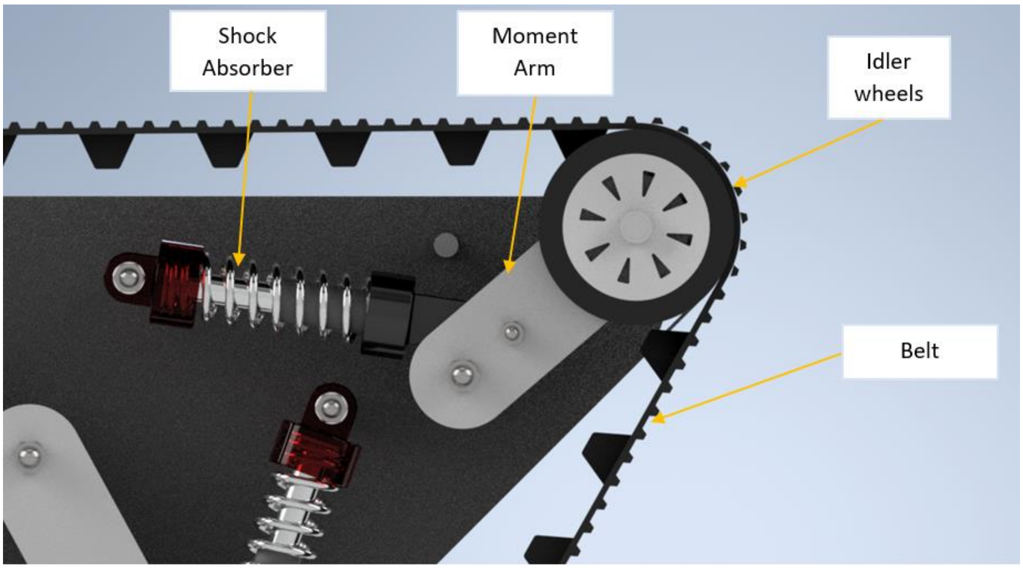

Figure 5 *| Labelled Model of Tensioner Assembly*

To deal with this problem, most tracked robots have a tensioner assembly fitted at its rear end. Under normal static conditions the shock absorber in the tensioner assembly is in a pre-compressed state, hence, pressing the idler wheels against the belt. When in motion the suspension of the track assembly experiences compressions and thus reducing the loop length for the belt. To counter this reduction in loop length, the pre-compressed shock absorber of the tensioner assembly extends and presses the idler wheels of the assembly against the belt. Thus, maintaining the necessary tension in the belt for it to not come off.

4.2 Drive Wheel

The drive wheel of the track mechanism is driven from the drive shaft via chain sprocket mechanism. The drive wheel is designed such that it has equally spaced cutouts to accommodate the protrusions from the belt. The belt on the other hand has protrusions that can perfectly fit into the cut outs on the drive wheel. The mating of the belt and drive wheel is responsible for moving the whole vehicle once the power is provided to the drive wheel. Flanges on either side of the drive wheel stop the belt from sliding on the drive wheel. An image of the drive wheel and the belt assembly is shown in Figure 6:

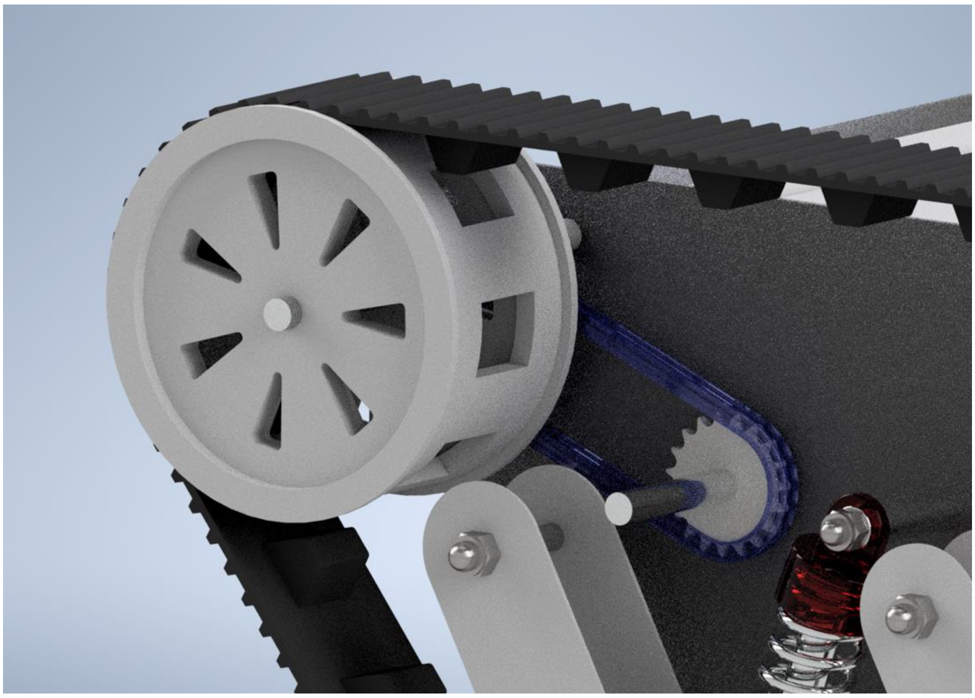

Fig. 6. *Belt and Drive Wheel Assembly*

4.3 Overall Assembly:

There are several other small components that are mandatory for the assembly and functioning of the track mechanism which include:

- Shafts for all the arms, shock absorbers and drive wheels which attach them to the main body.
- Nuts and bolts as per requirement for the assembly of various components.
- Bearings for fitting all the rotating shafts. Mounted bearings are used for fitting bearings to the plates.

It is to be noted that the track mechanism is repetitive assembly of the above-mentioned components. Apart from the main body all the components have their mirrored counter parts at the opposite side of the assembly. Assembling all the parts together gives us a complete assembly as shown in Figure 7. In the current configuration the track mechanism has a ground clearance of 355.600 mm and an angle of attack of 52.380 degrees. The gap between the consecutive idler wheels is 304.800 mm.

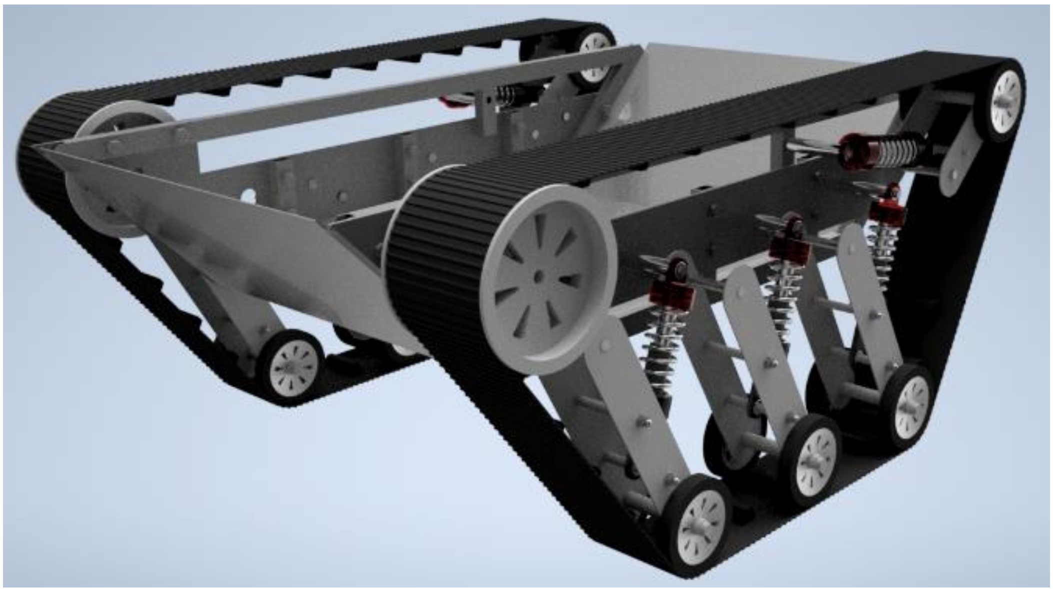

Fig. 7. *Complete Assembly*

Table 2: Main Design Parameters

Sr. No.	Parameter	Value
i.	Length	1530 mm
ii.	Width (along with wheel and track belt)	914 mm
iii.	Frame Width	558 mm
iv.	Height	658 mm
v.	Diameter of Driving Wheel	210 mm
vi.	Thickness of Driving Wheel	102 mm
vii.	The gap between the consecutive idler wheels	304.800 mm.
viii.	Ground Clearance	355.600 mm
ix.	Angle of Attack	52.380 degrees
x.	Body Weight	95 kg
xi.	Load Capacity	50 kg
xii.	Wheel Diameter	125 mm
xiii.	Wheel Thickness	30 mm

5. Analysis of Track Mechanism

5.1 Structural Analysis

i. Frame and Side Plates

The overall assembly was tested in ANSYS static structural module for the total deformation and maximum stress. A loading condition of 200 N bearing was applied to all the holes for legs and suspension. Thus, the total vertical load on the frame assembly amounted to 1200 N. The graphic in Figure 8 shows the total deformation of the frame assembly.

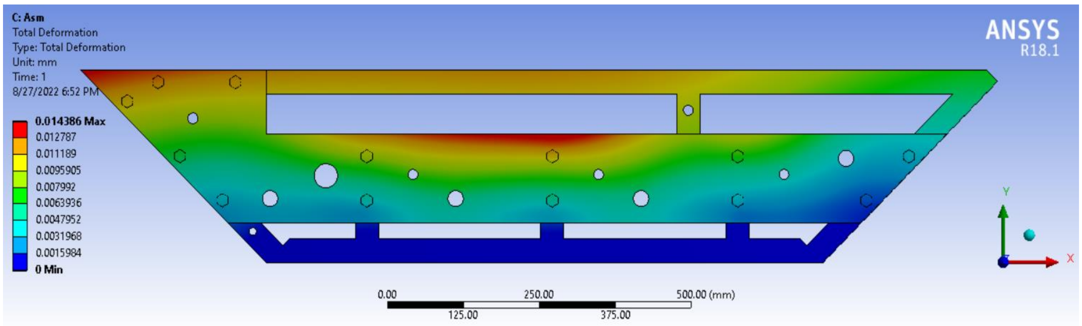

Fig. 8. *Total Deformation of Frame and Plates Assembly*

The maximum total deformation under the given loading came out to be 0.014 mm which is quite small and in a non-critical region of the structure. The maximum principal stress came out to be 8.946 MPa. The principal stress varied with in a band of 8.946 MPa to -2.176 MPa across the structure and can be seen in Figure 9:

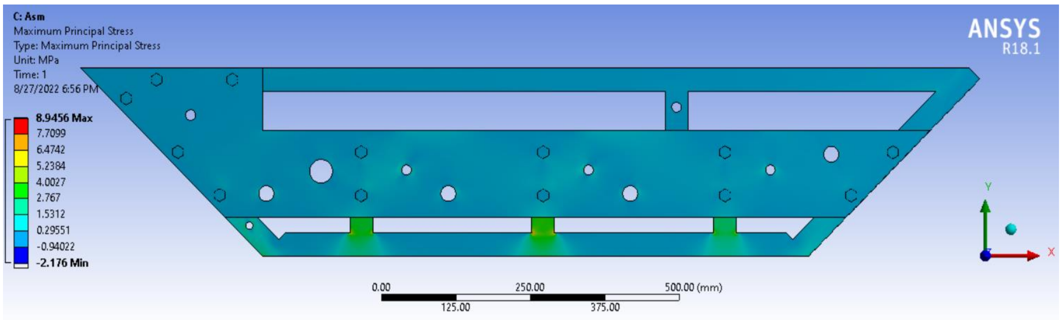

Fig. 9. *Maximum Principal Stress of Frame and Plates Assembly*

The factor of safety for the structure came out to be 9.189 which is well within safety limits.

ii. The Idler Assembly

The idler assembly was subjected to the estimated loading condition of 245 N on the wheels. The upper end at the shaft was fixed and the analysis was run for total deformation and maximum principal stress. The graphic in Figure 10 shows the maximum principal stress for the idler assembly:

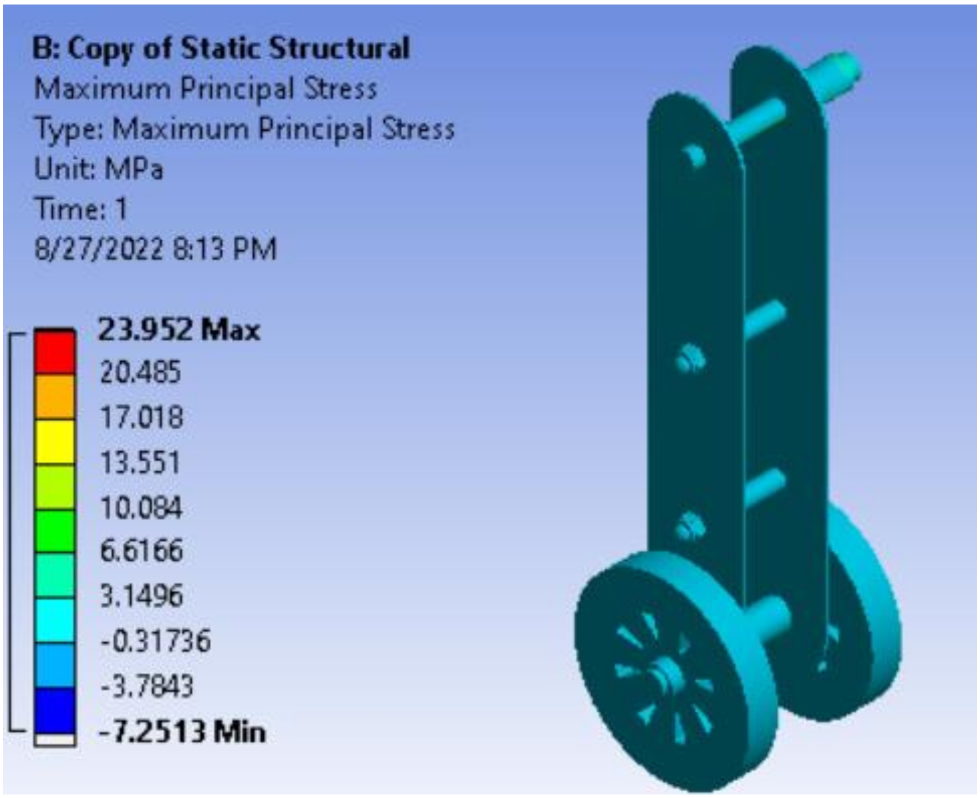

Fig. 10. *Maximum Principal Stress of Idler Assembly*

The maximum principal stress comes out to be 23.952 MPa and the stress varies within a band of -7.251 MPa to 23.952 MPa across the assembly (Figure 10). The maximum total deformation for the assembly came out to be 0.266 mm and the minimum safety factor was 11.710. Figure 11 shows the deformation of the assembly.

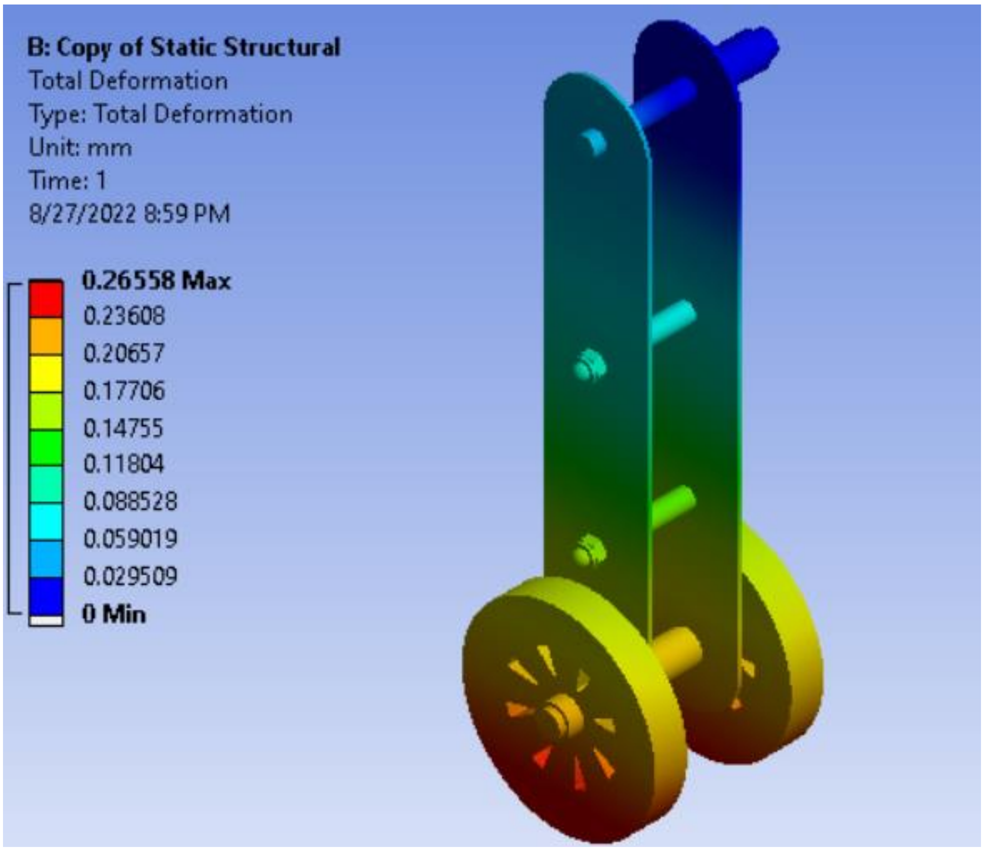

Fig. 11. *Total Deformation of Idler Assembly*

iii. Shock Absorber

A working load of 250 N was applied to the shock absorber's upper end while the lower end was fixed. The maximum deformation observed was 15.921 mm as shown in Figure 12.

The spring constant thus comes out to be 15.700 N/mm, which in comparison to the analytical results is within ~16 percent of the analytical results and is quite acceptable. The graphic in Figure 12 shows the total deformation of the shock absorber.

The stress distribution across the shock absorber assembly varied with in a range of -15.054 MPa to 156.55 MPa. The larger values are due to the large deformations of the spring. Overall, the shock absorber assembly is within the requirements of our loading condition.

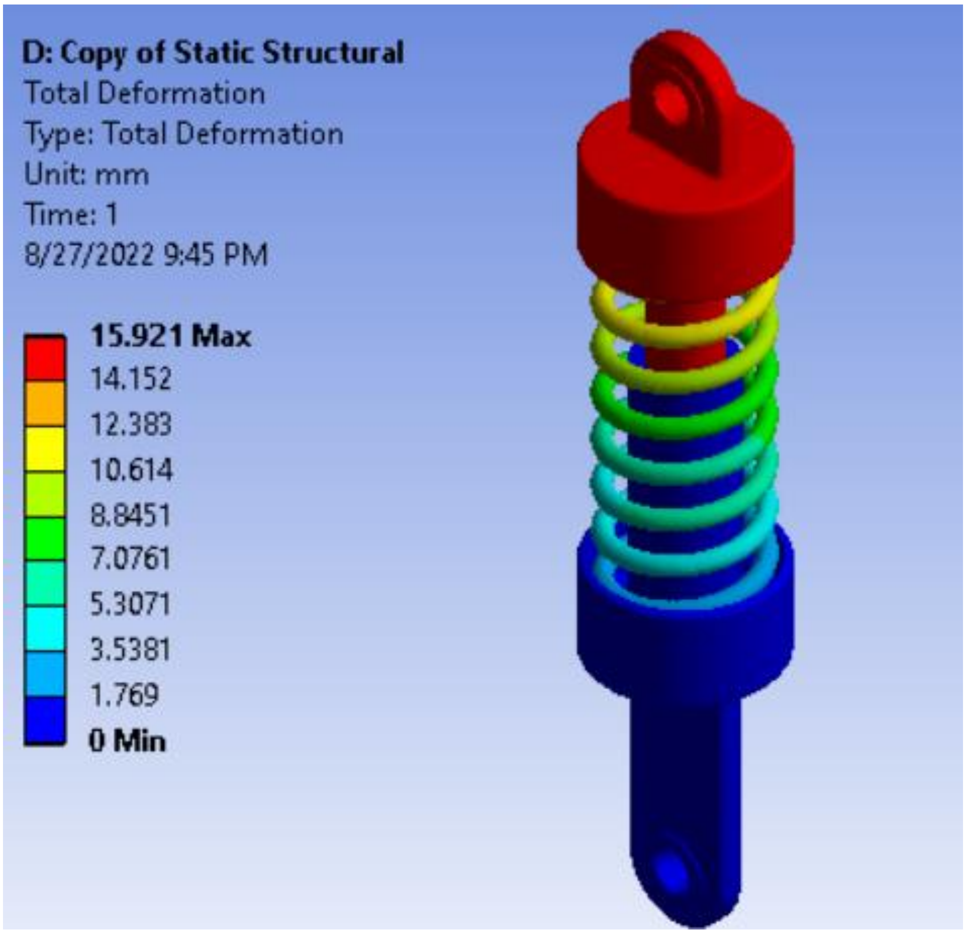

Fig. 12. *Total Deformation of Shock Absorber Assembly*

5.1 Simulation in V-REP

The proposed design of the track mechanism was simulated in CoppeliaSim to check if it can cope with the obstacles such as stairs and other obstacles such as cylindrical obstacles.

The model had to be replicated in CoppeliaSim. Keeping in view limitations of the software certain amendments had to be made to make a closest replica of the track mechanism in CoppeliaSim.

- Parts were recreated in the software itself with the same dimensions and using pure shapes such as cylinders, spheres, and cuboids.
- Revolute joints were used at all the locations where rotation was expected such as wheels, ends of shock absorber and legs.
- Prismatic joints in spring damper mode were used to imitate shock absorbers.
- A series of linkages were used joined by revolute joints to mimic the belt used in the design.
- Power was provided to the drive wheel in torque force mode, while the remaining wheels ran as idlers.

The model thus generated in the CoppeliaSim is as follows in Figure 13:

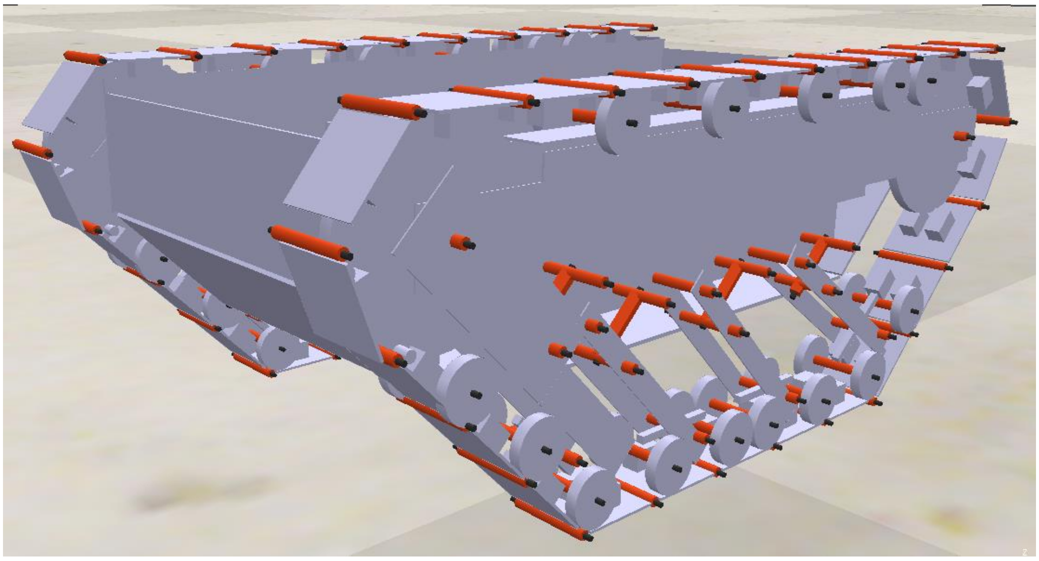

Fig. 13. *Model Generated in CoppeliaSim*

After generating the model in CoppeliaSim, it as tested against different obstacles; the results of which are discussed below:

i. Over a Cylinder

In the first simulation, the model was tested over a horizontal cylindrical obstacle. The height of the obstacle was kept 1.5 ft. as the limiting height of obstacle. The track mechanism performed as expected and crossed the obstacle easily. An image of robot over the obstacle is shown in Figure 14:

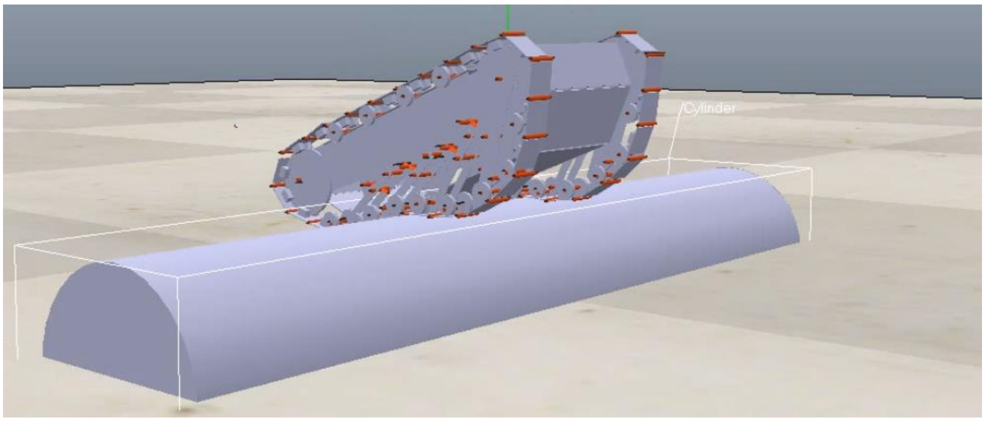

Fig. 14. *Simulation Over a Cylindrical Obstacle*

ii. Stair Climbing

In the next simulation, the model was tested against a set of stairs and was checked if the design could deal with a set of 1ft high stairs. In the simulation the track mechanism performed as expected and was able to deal with the set of stairs with ease. An image of the climb is shown here in Figure 15 while the robot was midway in its climb.

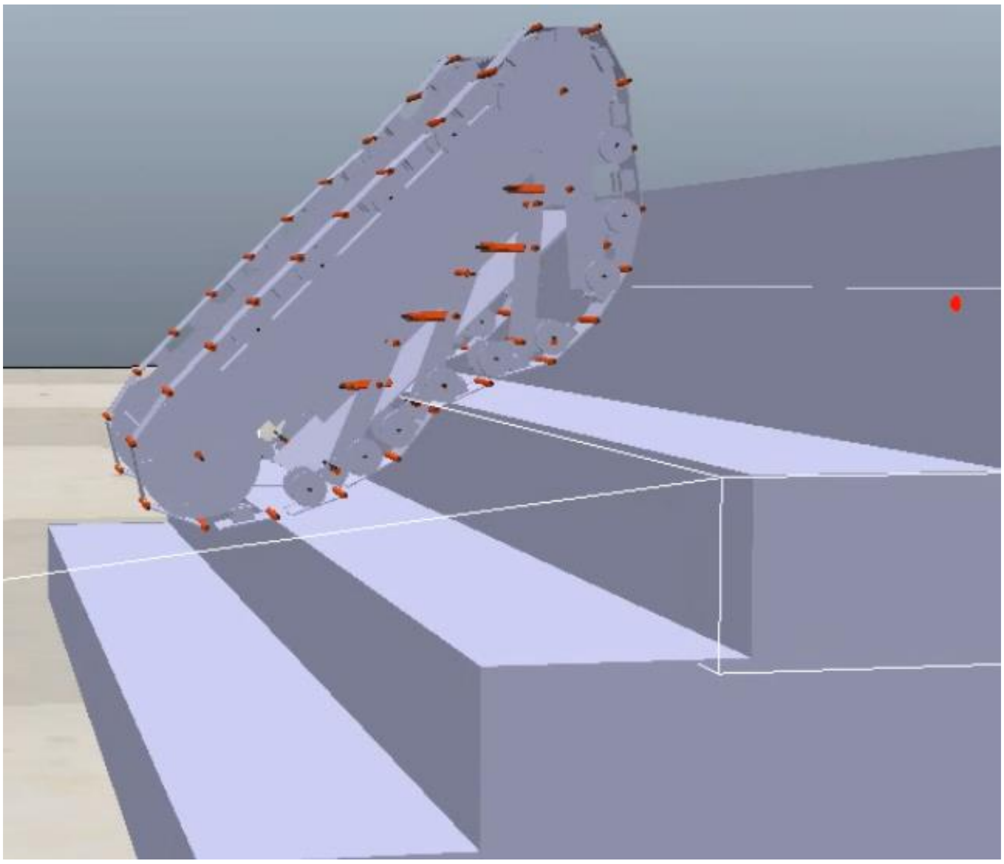

Fig. 15. *Stair Climbing in CoppeliaSim*

iii. Over a Series of Cylinders

In the next simulation, the model was tried over a series of cylinders 1.5ft high. This simulation was run to test the limiting climb height of the robot. The model climbed over the series of cylinders easily shown in Figure 16. The robot had a bumpy exit from the series of cylindrical obstacles due to the fact that this was the almost the limit beyond which it would topple. An image of robot over the obstacles is shown:

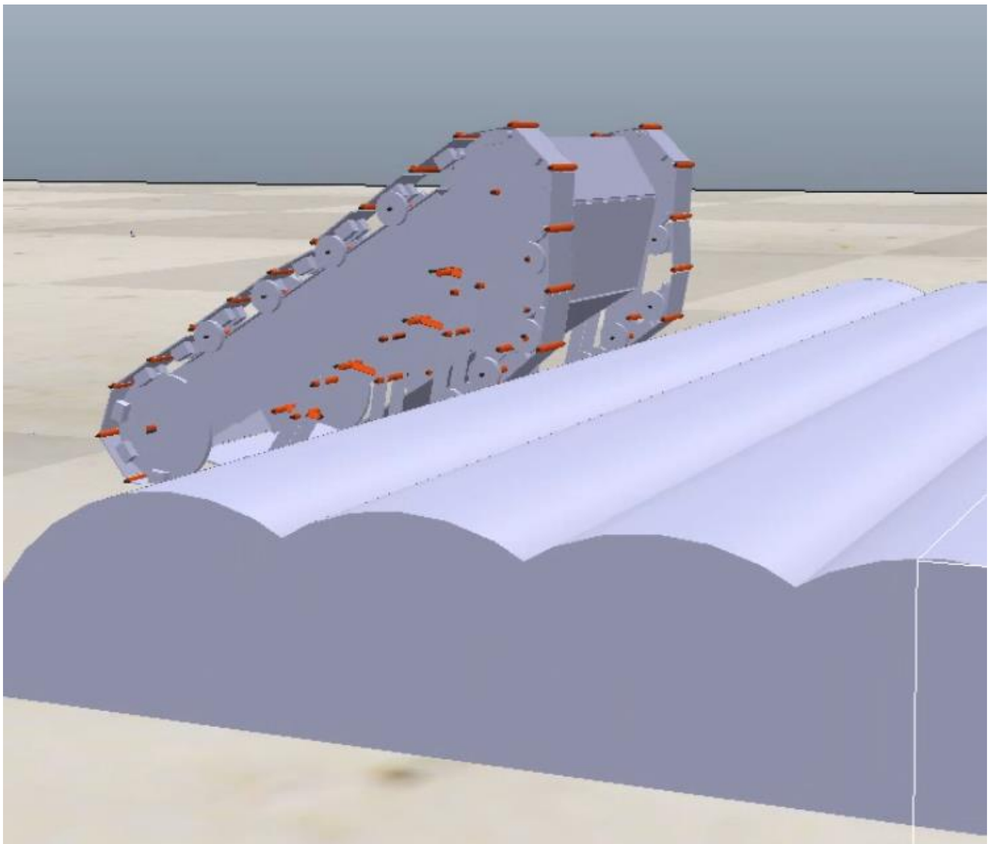

Fig. 16. *Obstacle Tackling in CoppeliaSim*

From the simulations the performance of the track mechanism against different obstacles is satisfactory and it is verified that the different set perimeters set for the track mechanism are working well in the simulation environment.

6. Fabrication

From the results it is evident that the designed track mechanism would serve its intended purpose. With ample ground clearance and the larger entrance angle, it would be able to tackle harsh terrains and difficult obstacles that may come in its way. The proposed design is now ready for fabrication stage.

Figure 17 *| Fully Assembled Chassis and Track Mechanism*

Fig. 18. *Side View of Complete Assembly*

Material and parts were procured as per requirement and availability. The track mechanism was then fabricated according to the design files. Minimal changes were accommodated in the fabricated model to overcome any limitations of ease of manufacturability. The fabricated model is shown in Figures 17 and 18:

7. Conclusion

From this reults of this study it is evident that the designed track mechanism can perform the desired functions for a supervised tele-operated firefighting robot over uneven terrains especially stair-like surfaces. The fabricated model, as explained in this study, is now ready for the installation of various components, like power unit, differential drive, hose manipulator, control system, and other functionalities. In the second phase testing of the track mechanism will be conducted once installation is completed. The entire system can be powered by an internal combustion engine, to transmit power to the differential drive mechanism proposed [21]. The power unit selected for the track mechanism is a 110-cc motorcycle engine, whose output, after passing through the reduction ratios of the differential drive, will be adequate to propel the mobile platform.

References

[1] T. N. Khoon, P. Sebastian, and A. B. S. Saman, "Autonomous firefighting mobile platform," *Procedia Engineering*, vol. 41, pp. 1145–1153, 2012.

[2] A. L. Shaikh, S. J. Shinde, and S. G., "Automated Fire Fighting Robot," *International Research Journal of Modern Engineering and Technology Science*, vol. 5, pp. 3090–3099, 2023.

[3] T. Anuradha and M. F. F. U. Khan, "Arduino controlled fire detection robot," *Technoarete Transactions on Advanced Computer Applications*, vol. 2, no. 2, pp. 1–5, 2023.

[4] J. Sathe, V. Raut, R. Peddapelli, J. Waghchaure, and V. W. Bembrekar, "Design and development of fire fighting robot," *International Research Journal of Engineering and Technology*, vol. 10, pp. 1753–1757, 2023.

[5] N. K. Choudhari, S. Ponnamanda, G. Deshbhratar, A. Gajbhiye, S. Chaudhari, and S. Harde, "Fire fighting robot," *International Journal of Scientific Research in Science, Engineering and Technology*, vol. 10, no. 2, pp. 514–518, 2023.

[6] J. Ma, J. Luo, H. Pu, and Y. Peng, “Design, simulation and manufacturing of a tracked robot for nuclear accidents,” *IEEE International Conference on Robotics and Biomimetics*, pp. 1828–1833, 2014.

[7] T. AlHaza, A. Alsadoon, Z. Alhusinan, M. Jarwali, and K. Alsaif, “New concept for indoor fire fighting robot,” *Procedia Social and Behavioral Sciences*, vol. 195, pp. 2343–2352, 2015.

[8] A. Ur Rehman, D. S. Necsulescu, and J. Sasiadek, “Robotic-based fire detection in smart manufacturing facilities,” *IFAC-PapersOnLine*, vol. 28, no. 3, pp. 1640–1645, 2015.

[9] S. Nurshuhada, M. L. F. Anis, J. Z. Ong, M. H. S.Nur, M. Z. S. Abdul, R. Nurul, Z. L. Hanisah, A. S. N. Wan, M. H. B. Nurul, and M. T. Hazwan, “Autonomous robotic fire detection and extinguishing system,” *Journal of Physics: Conference Series*, vol. 2107, pp. 1–8, 2021.

[10] J. Cui, Y. Wang, A. Li, S. Shao, and X. Cai, “Design and analysis of tracked robot with differential mechanism,” *Proceedings of the IEEE Conference on Industrial Electronics and Applications*, pp. 829–832, 2018.

[11] M. Rajesh, R. Karthikeyan, P. Arunkumar, S. Jeeva, and S. Srinivasan, “Design and development of an industrial firefighting rover,” *Materials Today: Proceedings*, vol. 45, pp. 7965–7969, 2021.

[12] N. M. A. M. Najm, A. K. Hussain, S. I. Mustafa, and B. Rashit, “Design and implementation of a robot firefighter for indoor applications,” *Proceedings of the FRUCT Conference*, vol. 35, pp. 482–491, 2024.

[13] P. Singh, A. Solanki, P. Paras, D. Soni, P. Bhavsar, S. Dubey, “Design and analysis of mini fire fighting robot,” *International Journal of Research in Applied Science and Engineering Technology*, vol. 10, no. 11, pp. 1037–1041, 2022.

[14] X. Duan, Q. Huang, &N. Rahman, J. Li, J. Li, “MOBIT, a small wheel-track-leg mobile robot,” *Proceedings of the World Congress on Intelligent Control and Automation*, vol. 2, pp. 1–8, 2006.

[15] P. Ben-Tzvi, A. A. Goldenberg, and J. W. Zu, “Design, simulations and optimization of a tracked mobile robot manipulator with hybrid locomotion and manipulation capabilities,” *Proceedings of the IEEE International Conference on Robotics and Automation*, pp. 2307–2312, 2008.

[16] Z. Y. Chen, G. Z. Chen, L. Z. Qi, F. Yin, D. D. Li, and M. J. Shi, “Steering dynamic performance analysis of the tracked mobile robot,” *Materials Science and Engineering*, vol. 392, no. 6, pp. 1–8, 2018.

[17] W. Tao, Y. Ou, and H. Feng, “Research on dynamics and stability in the stairs-climbing of a tracked mobile robot,” *International Journal of Advanced Robotic Systems*, vol. 9, pp. 1–8, 2012.

[18] J. Matej, “Tracked mechanism simulation of mobile machine in MSC.ADAMS/View,” *Research in Agricultural Engineering*, vol. 56, pp. 1–7, 2010.

[19] G. Tao, G. Jun, H. Bo, P. Huadong, “Power consumption of tracked and wheeled small mobile robots on deformable terrains—model and experimental validation,” *Mechanism and Machine Theory*, vol. 133, pp. 347–364, 2019.

[20] M. M. Dar, N. Rahman, and R. A. Mufti, “Steering mechanism for an IC engine powered tracked firefighting UGV,” *University of Wah Journal of Science and Technology*, vol. 5, pp. 41–46, 2021.